Current Biology 17, 947–952, June 5, 2007 ©2007 Elsevier Ltd All rights reserved DOI 10.1016/j.cub.2007.04.038

Report

A Novel ROP/RAC Effector Links Cell Polarity, Root-Meristem Maintenance, and Vesicle Trafficking

Meirav Lavy,[1,2] Daria Bloch,[1,2] Ora Hazak,[1,2] Itai Gutman,[1] Limor Poraty,[1] Nadav Sorek,[1] Hasana Sternberg,[1] and Shaul Yalovsky[1,*]
[1] Department of Plant Sciences
Tel Aviv University
Tel Aviv 69978
Israel

Summary

ROP/RAC GTPases are master regulators of cell polarity in plants, implicated in the regulation of diverse signaling cascades including cytoskeleton organization, vesicle trafficking, and Ca^{2+} gradients [1–8]. The involvement of ROPs in differentiation processes is yet unknown. Here we show the identification of a novel ROP/RAC effector, designated interactor of constitutive active ROPs 1 (ICR1), that interacts with GTP-bound ROPs. ICR1 knockdown or silencing leads to cell deformation and loss of root stem-cell population. Ectopic expression of ICR1 phenocopies activated ROPs, inducing cell deformation of leaf-epidermis-pavement and root-hair cells [3, 5, 6, 9]. ICR1 is comprised of coiled-coil domains and forms complexes with itself and the exocyst vesicle-tethering complex subunit SEC3 [10–13]. The ICR1-SEC3 complexes can interact with ROPs in vivo. Plants overexpressing a ROP- and SEC3-noninteracting ICR1 mutant have a wild-type phenotype. Taken together, our results show that ICR1 is a scaffold-mediating formation of protein complexes that are required for cell polarity, linking ROP/RAC GTPases with vesicle trafficking and differentiation.

Results and Discussion

To identify novel ROP/RAC-interacting proteins, a constitutive-active Atrop10^{CA}/Atrac8^{CA}) was used as bait in yeast two-hybrid screens. Two proteins comprised of 343 and 584 amino acids that were designated interactor of constitutive active ROP1 and 2 (ICR1 and ICR2), respectively, were identified. Sequence analysis showed that ICR1 (At1g17140) and ICR2 (At2g37080) share 20% overall similarity and are comprised almost entirely of coiled-coil domains and no other recognized catalytic or structural domains (Figure S1 in the Supplemental Data available online). ICR1 shows 23% identity and 47% similarity to Rho-associated coiled-coil making protein kinase 1 (ROCK1) [14].

To study the function of ICR1 in plants, a T-DNA insertion mutant (*icr1*$^{-/-}$) (SAIL_265_G05) has been identified [15]. The T-DNA insertion is located in the 5′-UTR of *ICR1*, 186 bp upstream of the initiation codon (Figure 1A). *ICR1* mRNA is alternatively spliced at the 5′-UTR, yielding two transcripts, which have the same ORF (Figures 1A and 1B and GenBank accession numbers At1g17140.1 and At1g17140.2). Both transcripts could not be amplified in the mutant (Figure 1B). However, low levels of a shorter transcript containing the entire *ICR1* ORF could still be amplified by RT-PCR from RNA isolated from seedlings (Figure 1C).

The adaxial epidermal pavement cells of *icr1* mutant plants are cubical (Figure 1E) and not interdigitated lobed like wild-type cells (Figure 1D) or elongated noninterdigitated like *ICR1*-overexpressing cells (Figure 1R). Interestingly, trichome development and abaxial epidermis cell shape were not altered in the mutant, indicating either that ICR1 affects growth of only certain epidermal cells or that expression of the shorter *ICR1* transcript was sufficient to maintain normal growth of some cells. In segregating populations (100 seedlings), this mutant phenotype segregated in a 1 to 3 ratio, strictly cosegregating with the *T-DNA* insert in the *ICR1* UTR and the *Bar* gene selection marker. A Southern blot analysis revealed only a single *T-DNA* insertion in a homozygous *icr1* genome (Figure S2). To assess the interaction between *ICR1* and *ROPs*, the *icr1* mutant was crossed with a *GFP-Atrop6*^{CA}/*Atrac3*^{CA}-overexpressing line. Overexpression of GFP-Atrop6^{CA}/Atrac3^{CA} induces development of rectangular rather than lobed interdigitated leaf-epidermis-pavement cell (Figure 1G). The adaxial epidermis cells of the *icr1 GFP-Atrop6*^{CA}/*Atrac3*^{CA} plants resembled more cells of the *icr1* single mutant (Figure 1F) and differed from the rectangular *GFP-Atrop6*^{CA}/*Atrac3*^{CA} cells (Figure 1G). This nonadditive phenotype suggested that a wild-type ICR1 is required for AtROP6 gain of function.

icr1$^{-/-}$ plants had short primary roots that reached a maximal length of up to 0.5 cm and then ceased growth and developed numerous adventitious roots (Figure 1H). This phenotype suggested that the root apical meristem collapsed. 25 independent *ICR1-RNAi* (*icr1*^{sil}) lines were analyzed to further determine whether the phenotype detected for *icr1*$^{-/-}$ T-DNA mutant plants is associated with *ICR1* loss of function. Three representative independent *icr1*^{sil} lines are shown (Figures 1M–1O; Figure S3). Similar to the *icr1*$^{-/-}$ T-DNA mutant plants, the *icr1*^{sil} lines developed numerous adventitious roots and had short primary roots (compare Figures 1H and 1M and Figures S3A–S3D). In both the *icr1*$^{-/-}$ and *icr1*^{sil} lines, the adventitious roots collapsed after reaching a length of 2–3 cm. This indicates that ICR1 is required for primary and adventitious root maintenance but not for their formation. Development of root hairs at the root tip and the differentiation and organization of columella cells are two morphological indicators that have been associated with dysfunction of the root meristem [16, 17]. In both *icr1*$^{-/-}$ (Figure 1J) and *icr1*^{sil} (Figures 1N and 1O; Figures S3F and S3G) plants, root hairs developed close to the root tip, indicating that the cells attained a mature epidermal identity [16]. The

*Correspondence: shauly@tauex.tau.ac.il
[2] These authors contributed equally to this work.

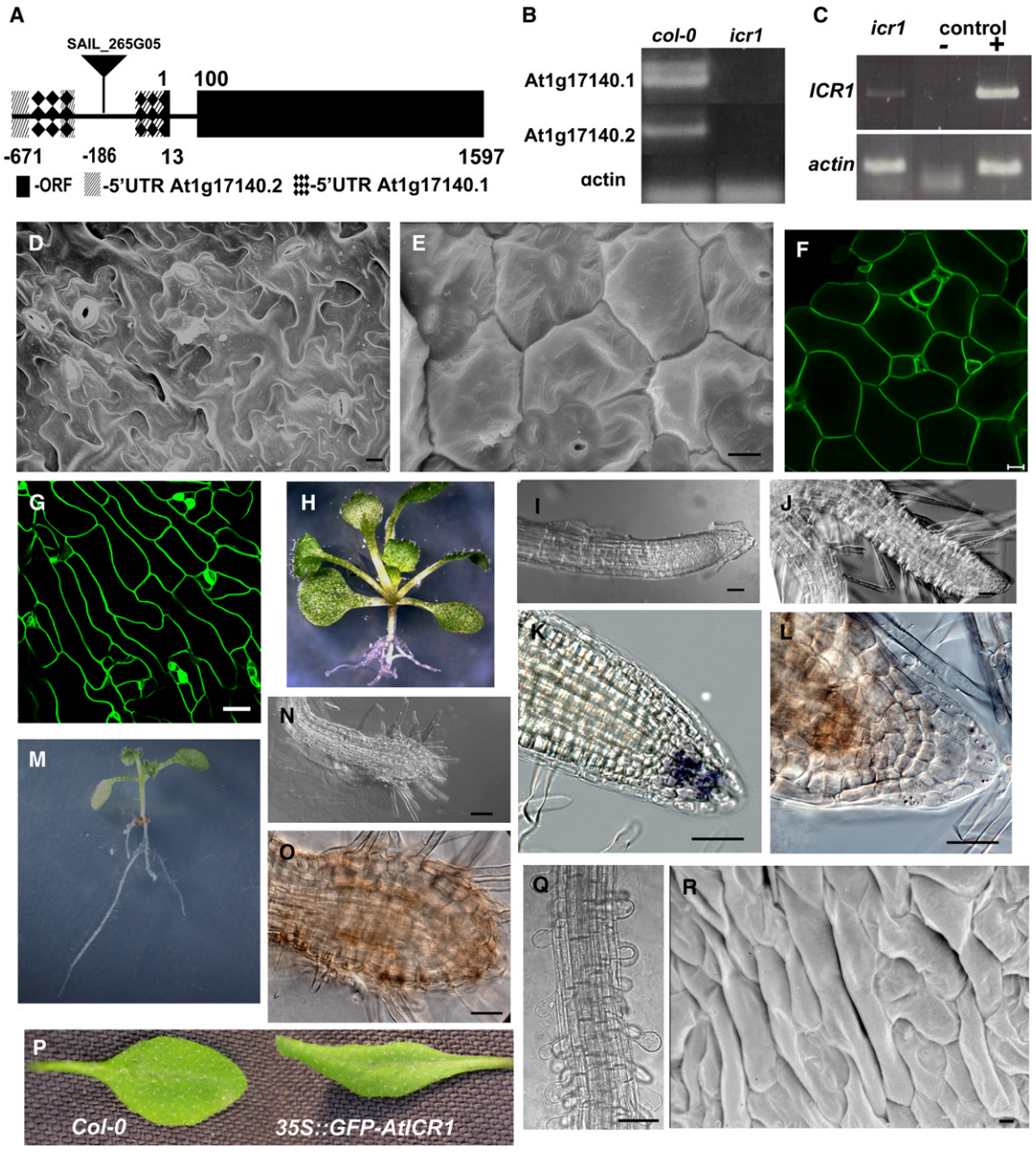

Figure 1. *ICR1* Mutant and Overexpression Phenotypes

(A) A schematic representation of *ICR1* transcripts and T-DNA insertion site.

(B and C) RT-PCR of full-length *ICR1* transcripts (*At1g17140.1* and *At1g17140.2*) with primers amplifying fragments initiating at positions −651 and −487 bp upstream of the initiation AUG codon, specific for either transcript (B), and a primer initiating at −91 bp upstream of the initiation AUG codon to amplify the *ICR* ORF (C). Control: *Col-0* RNA (+) and no RNA (−).

(D–G) Leaf-epidermis-pavement cells of *Col-0* (D), *icr1*$^{-/-}$ (E), *icr1*$^{-/-}$ *GFP-Atrop6*^{CA} (F), and *GFP-Atrop6*^{CA} (G) plants.

(H) An *icr1*$^{-/-}$ plant with a short primary root and an excess of adventitious roots.

(I and J) Root tips of wild-type *Col-0* (I) and *icr1*$^{-/-}$ (J) seedlings at 14 days after germination. Note the root hairs close to the root tip in the *icr1*$^{-/-}$.

(K and L) Iodine (lugol) stain of starch granules of wild-type *Col-0* (K) and *icr1*$^{-/-}$ (L) roots. Note the absence of the lugol-stained starch granules, irregular cell-division planes, and swelling of the *icr1*$^{-/-}$ root tip.

(M–O) An *ICR1-RNAi* (*icr1*^{sil}) seedling and root tip.

(M) An *icr1*^{sil} seedling with a short primary root and numerous adventitious roots.

(N) The root tip of the primary root of the *icr1*^{sil} seedling shown in (M). Note the swollen root and root-hair development at the root tip.

(O) The same root tip as in (N) after lugol staining. Note the absence of starch granules.

(P) Rosette leaves of *Col-0* and transgenic *GFP-ICR1* plants.

(Q and R) Swollen root hairs (Q) and deformed leaf-epidermis-pavement cells (R) of *GFP-ICR1* plants.

Scale bars represent 20 μm in (D)–(G), (I)–(L), (N), and (O) and 10 μm in (Q) and (R).

columella identity was examined by staining starch granules. Lugol-stained starch granules were observed in columella cells of WT roots (Figure 1K, dark stain). In contrast, lugol-stained starch granules were not observed in primary roots of *icr1*$^{-/-}$ (Figure 1L) and *icr1*^{sil} (Figure 1O; Figures S3I and S3J) plants. The root tips of *icr1*$^{-/-}$ mutant (Figure 1L) and *icr1*^{sil} (Figures 1N and 1O; Figures S3I and S3J) seedlings were swollen and irregular cell-division planes were observed.

Taken together, the data in Figure 1 and Figure S3 indicated that loss of *ICR1* function leads to collapse of the root meristem. The *icr1*$^{-/-}$ mutant and *icr1*^{sil} lines were partially male sterile, indicating that pollen development too was compromised.

Plants overexpressing GFP-ICR1 were virtually indistinguishable from plants that overexpress activated ROPs. The rosette leaves had longer petioles, their blades were folded downward (Figure 1P; Figure S4), and the root hairs were swollen (Figure 1Q). The epidermal pavement cells were rectangular and not interdigitated and lobed (Figures 1R and 1G), suggesting that ICR1 is indeed a ROP effector. Next, the interactions between ROPs and ICR1 were studied in detail to explore the functional relation between the proteins.

Qualitative and quantitative yeast two-hybrid assays showed that either WT or constitutive active (CA) forms of AtROP6/AtRAC3 and AtROP10/AtRAC8 but not a dominant-negative (DN) AtROP10/AtRAC8 mutant interacted with ICR1 (Figures 2A and 2F). In vitro pull-down assays of His_6-AtROP6 with GST-ICR1 demonstrated the physical interaction between the two proteins and that ICR1 preferentially interacted with GTP-bound ROPs (Figures 2B and 2E). In the presence of up to 5 μg of either GST or GST-ICR1 in the pull-down mixtures, precipitation of His_6-ROP6/RAC3 has been detected only with the ICR1 fusion protein. At 10 μg of GST, some nonspecific interaction was detected but the interaction with GST-ICR1 was stronger (Figure 2E), confirming the specificity of the interaction between the ROP/RAC and ICR1.

ICR1 formed homo-oligomers but did not interact with ICR2 (Figure 2C). The homo-oligomerization of ICR1 was verified by pull-down of *E. coli*-expressed His_6-ICR1 and *Arabidopsis*-expressed YFP-ICR1 by GST-ICR1 (Figure 2D).

Next we examined the interaction between ROPs and ICR1 in plants. The interaction between ROPs and ICR1 in plants was demonstrated by bimolecular fluorescence complementation (BiFC) [18] and colocalization assays. After transient expression in *Nicotiana benthamiana* (*N. benthamiana*) leaf epidermis, both the type I (AtROP6/AtRAC3) and the type II (AtROP10/AtRAC8) ROPs interacted with ICR1 in the plasma membrane (Figures 2G and 2H). When ICR1 was coexpressed with ROP lipid acceptor mutants, Atrop6mS/Atrac3mS and Atrop10mSS/Atrac8mSS [19, 20], the reconstituted YFP complexes were observed in nuclei (N) and cytoplasmic strands (CS) (Figures 2I and 2J). This indicated that the localization of the ICR1-ROP complexes at the plasma membrane depended on the lipid modifications of the ROPs. No YFP fluorescence was detected in negative control experiments in which either YN-ICR1 or YC-ICR1 were coexpressed with a corresponding empty vector control or with dominant-negative ROP mutants (data not shown). GFP-ICR1 was colocalized with mRFP-Atrop11^{CA}/Atrac10^{CA} in the plasma membrane of double transgenic plants (Figures 2K–2N; Figures S5 and S6). After plasmolysis, GFP-ICR1 and mRFP-Atrop11^{CA}/Atrac10^{CA} were observed on cell-wall-detached plasma membrane (Figure 2N). In nonplasmolyzed cells, the cytoplasm is pressed against the membrane, making it difficult to discern between membrane-localized and -nonlocalized protein. Membrane floatation centrifugation was used to further verify that when coexpressed with an activated ROP, GFP-ICR1 was attached to the membrane (Figure S5), like ROPs [6, 21]. The data in Figure 2 and Figures S5 and S6 indicated that type I and type II ROPs/RACs can interact with ICR1 and that this interaction likely takes place at or near the plasma membrane.

We suspected that ICR1 functions as a scaffold, mediating interactions of ROPs with different proteins. Yeast two-hybrid screens with ICR1 as bait were performed to identify ICR1 interactors. One of the proteins identified was the exocyst complex subunit AtSEC3A (At1g47550 [22, 23]). In yeast, Rho1 and Cdc42 interact with Sec3 [11, 24] and Rho3 interacts with the exocyst subunit Exo70 [25]. ICR1 but not ICR2 or different type I and type II ROPs interacted with AtSEC3A in yeast two-hybrid assays (Figure 3A). Furthermore, in the same assay, neither ICR1 nor ICR2 nor different ROPs interacted with an *Arabidopsis* EXO70 homolog (EXO70A1 [At5g03540] [22, 26]) (Figure 3A). The interaction of ICR1 with AtSEC3A required an intact C-terminal coiled-coil domain, similar to its interaction with ROPs (Figures 3B, 4A, and 4B). Pull-down assays of His_6-AtSEC3A with GST-ICR1 confirmed the physical interaction between the two proteins (Figure 3C). Next we examined whether ICR1 interacts with SEC3 in plants and whether ROPs and AtSEC3A could interact with ICR1 at the same time. BiFC assays demonstrated interaction of YN-ICR1 and YC-AtSEC3A (Figure 3D). Coexpression of YN-ICR1, YC-AtSEC3A, and CFP-ROP9/RAC7 resulted in colocalization of all three proteins in the plasma membrane (Figures 3F–3H). This suggests that both ROPs/RACs and AtSEC3A could interact with ICR1 at the same time.

ICR1 is predicted to contain two coiled-coil domains. Disruption of either domain interfered with the oligomerization of ICR1, but only disruption of the C-terminal (not the N-terminal) domain inhibited the interaction with ROPs (Figures 4A and 4B). The selection of mutated residues was based upon sequence conservation between ICR1 and ICR2. To establish a connection between the role of ICR1 in regulation of cell polarity and its interaction with ROPs and SEC3, transgenic plants expressing the icr1mPP$^{265, 270}$, a ROP/RAC- and SEC3-noninteracting mutant (Figures 4A, 4B, and 3B), were analyzed. An immunoblot showed that *GFP-icr1mPP*$^{265, 270}$ and GFP-ICR1 were expressed at similar levels (Figure 4C). The phenotype of the *GFP-icr1mPP*$^{265, 270}$ plants resembled that of wild-type plants (Figures 4D and 4E; Figure S7). The leaf-epidermis-pavement cells were interdigitated lobed (Figure 4D) and root hairs were elongated and not swollen (Figure 4E). These results strongly suggested that ICR1 function depends on its ability to interact with ROPs and/or SEC3.

In yeast, Rho1 and Cdc42 interact directly with Sec3 and induce its recruitment to the plasma membrane to

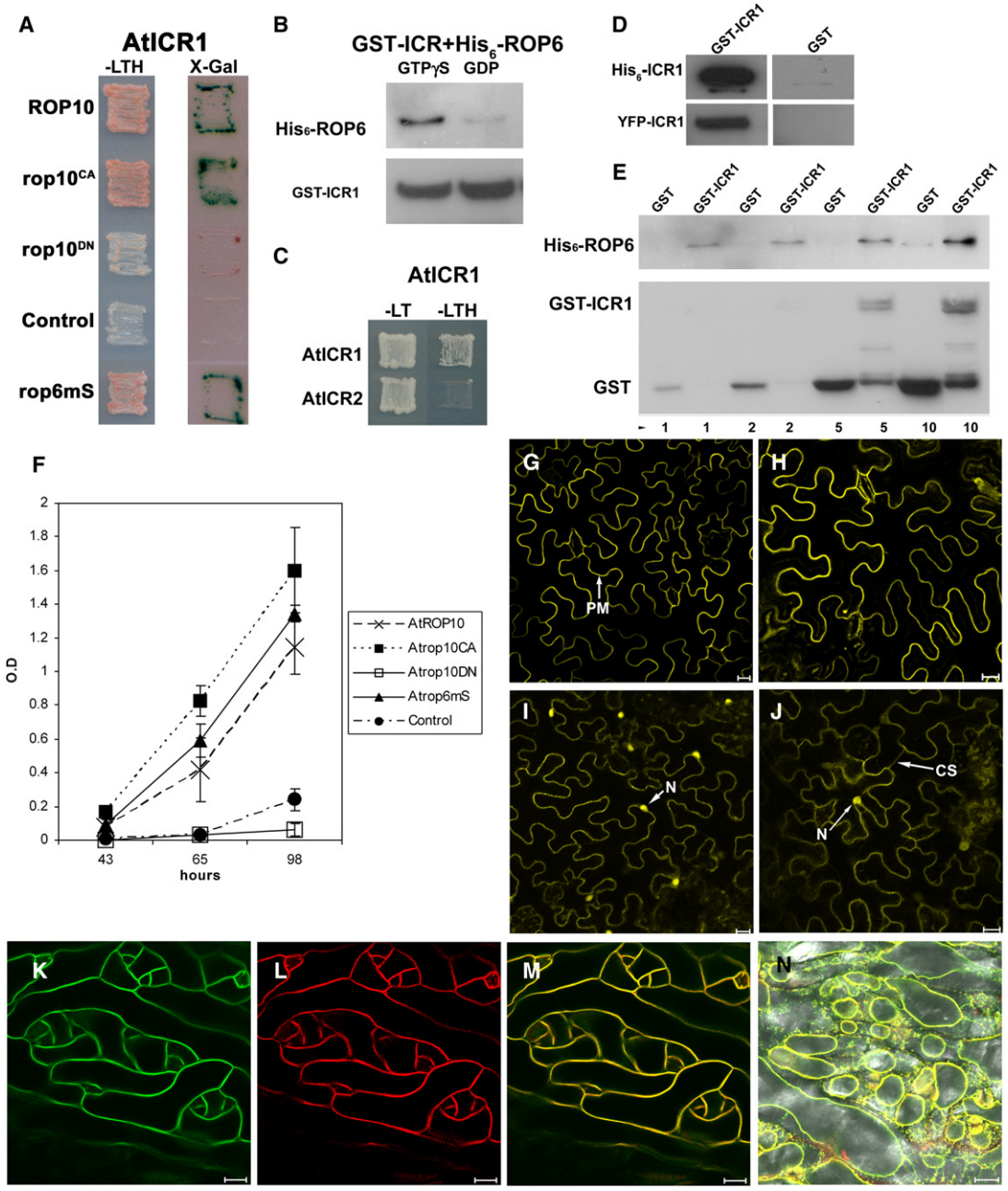

Figure 2. Interaction and Colocalization of ICR1 and ROPs

(A) Yeast two-hybrid assays. Abbreviations: −LTH, Leu, Trp, His-depleted media; Control, empty pGAD vector; rop6mS, a prenylation-deficient mutant in which the prenyl acceptor cysteine was mutated into serine.

(B) Pull-down of GTPγS- or GDP-loaded His_6-ROP6 by GST-ICR1 (top) and GST-ICR1 input (bottom).

(C) Yeast two-hybrid assays of ICR1 with itself and with ICR2.

(D) Pull-down with GST-ICR1 of *E. coli* expressed and purified His_6-ICR1 or YFP-ICR1 from *Arabidopsis* protein extracts.

(E) Pull-down of His_6-ROP6 with increasing amounts of GST or GST-ICR1 detected with α-His_6 (top) and α-GST (bottom) Abs. Numbers on bottom denote μg GST or GST-ICR1.

(F) Quantitative yeast two-hybrid assays performed by growing yeast on selective −LTH liquid medium supplemented with 3-AT. Experiments were carried out in triplicate. Bars represent standard error. The differences in growth rate between AtROP10, $Atrop10^{CA}$, Atrop6ms, and the $Atrop10^{DN}$ and empty vector controls were significant $p \leq 0.001$ (two-way ANOVA).

(G–J) BiFC assays of YC-ICR1 with YN-ROP6 (G) or YN-ROP10 (H) and their nonlipid-modified mutants YN-Atrop6mS (I) and Atrop10mSS (J) carried in *N. benthamiana* leaves.

(K–N) GFP-ICR1 mRFP-$rop11^{CA}$ double-transgenic *Arabidopsis*. Green, GFP channel (K); red, mRFP channel (L); yellow, GFP/mRFP overlay (M) and after plasmolysis (N). PM, plasma membrane; N, nuclei; CS, cytoplasmic strands.

Scale bars represent 20 μm in (G)–(N).

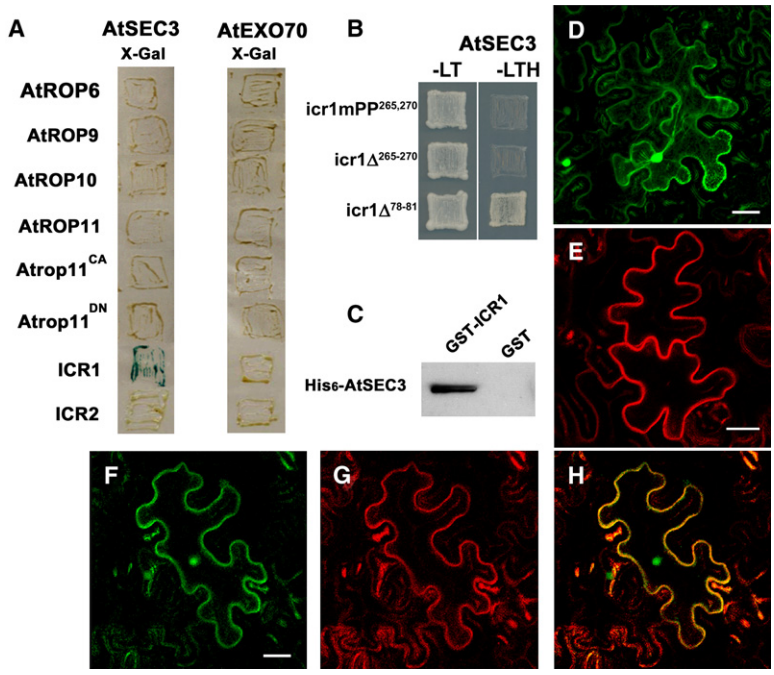

Figure 3. Interaction of ICR1 and AtSEC3A

(A) Yeast two-hybrid β-glucoronidase assays.

(B) Yeast two-hybrid assays of ICR1 mutants and AtSEC3A. Abbreviations: −LT/−LTH, Leu, Trp/Leu, Trp, His-depleted media.

(C) A protein immunoblot decorated with α-His_6 Abs of a pull-down of His_6-AtSEC3 with GST-ICR1.

(D) BiFC assays showing interaction of YN-ICR1 with YC-AtSEC3.

(E) Plasma-membrane localization of CFP-ROP9.

(F–H) Coexpression of YN-ICR1+YC-AtSEC3+CFP-ROP9. Green, YFP channel; red, CFP channel; yellow, overlay.

Scale bars represent 20 μm in (D)–(H).

facilitate polarized secretion [11, 24]. Another exocyst subunit, EXO70, interacts with the actin nucleation Arp2/3 complex, regulating cell migration [27] and linking secretion with actin organization. Plant and animal SEC3 homologs lack the yeast Sec3 Rho interaction domain. Our results suggest that in *Arabidopsis* ICR1 provides the missing link between Rho family GTPases and the exocyst. Development of root requires polar auxin transport that depends on distribution PIN family of auxin efflux carriers [28] and vesicle trafficking [29, 30]. Thus, ICR1 may provide a link between ROPs, the exocyst, vesicle trafficking, possibly actin nucleation, and auxin distribution.

Conclusions

ICR1 is a scaffold whose function is regulated by the ROP/RAC GTPase switch. The protein-interaction assays and mutant analysis indicate that ICR1 interacts with specific group of proteins and that at least part of its function is not redundant. Previously, a group of

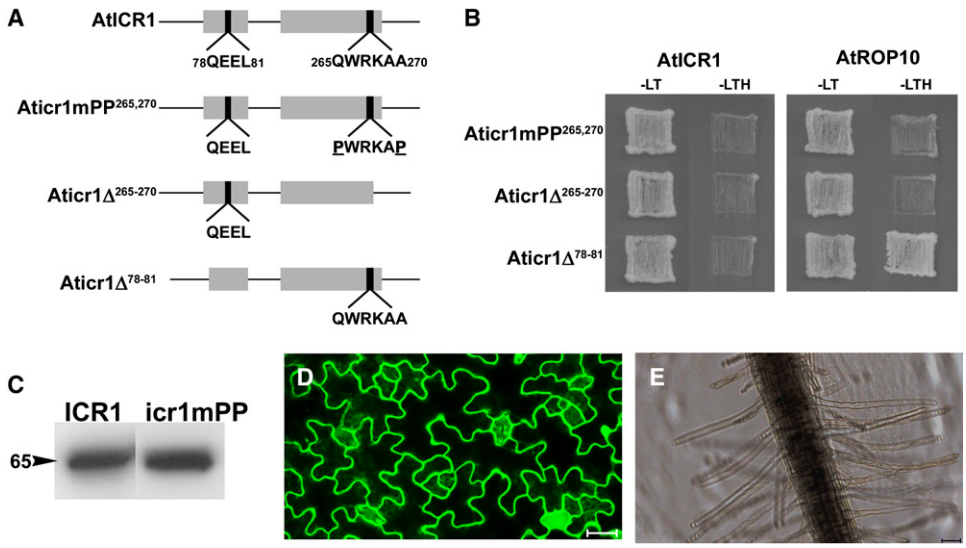

Figure 4. Interaction of ICR1 Mutants and Phenotype of *icr1mPP*^{265,270} Transgenic Plants

(A) Diagrams of site-specific mutants and deletions created in ICR1 N- and C-terminal coiled-coil domains. The mutated sequences in the WT protein are detailed in the upper diagram. Mutant proline residues are underlined.

(B) Yeast two-hybrid assays of the ICR1 mutant with themselves and with ROP10/RAC8. Abbreviations: −LT, medium lacking Leu and Trp; −LTH, medium lacking Leu, Trp, and His.

(C) Protein immunoblots decorated with α-GFP Abs of protein extracts from *GFP-ICR1* and *GFP-icr1mPP*$^{265, 270}$ plants.

(D and E) Interdigitated lobed leaf-epidermis-pavement cells (D) and elongated root hairs (E) that developed on *GFP-icrmPP*$^{265, 270}$ plants. Scale bars represent 20 μm.

CRIB-domain-containing ROP effector proteins designated RICs were identified and implicated in regulation of the cytoskeleton during growth of pavement cells and pollen tubes [7, 8]. ICR1 expands the plethora of ROP/RAC-regulated signaling and provides a convergence point for ROP/RAC-regulated pathways in cell polarity and differentiation. The ability of ICR1, ICR2, and possibly other coiled-coil domain proteins, which serve as binding platforms, to interact with various different proteins opens the door to elucidation of the complexity of ROP/RAC signaling.

Supplemental Data

Five tables, seven figures, and Experimental Procedures are available at http://www.current-biology.com/cgi/content/full/17/11/947/DC1/.

Acknowledgments

We thank D. Szymanski for comments and the *Arabidopsis* Biological Resource Center, University of Ohio for mutant seeds. This research was supported by the Israel Science Foundation Charles Revson research fund (ISF 399/03) and the German-Israeli DIP program to S.Y. M.L. was a recipient of the Israel Ministry of Science Eshkol and The Manna Center for Plant Biosciences, Tel Aviv University fellowships.

Received: January 21, 2007
Revised: April 14, 2007
Accepted: April 16, 2007
Published online: May 10, 2007

References

1. Nibau, C., Wu, H.M., and Cheung, A.Y. (2006). RAC/ROP GTPases: 'hubs' for signal integration and diversification in plants. Trends Plant Sci. *11*, 309–315.
2. Li, H., Shen, J.J., Zheng, Z.L., Lin, Y., and Yang, Z. (2001). The Rop GTPase switch controls multiple developmental processes in *Arabidopsis*. Plant Physiol. *126*, 670–684.
3. Molendijk, A.J., Bischoff, F., Rajendrakumar, C.S., Friml, J., Braun, M., Gilroy, S., and Palme, K. (2001). *Arabidopsis thaliana* Rop GTPases are localized to tips of root hairs and control polar growth. EMBO J. *20*, 2779–2788.
4. Fu, Y., Wu, G., and Yang, Z. (2001). Rop GTPase-dependent dynamics of tip-localized F-actin controls tip growth in pollen tubes. J. Cell Biol. *152*, 1019–1032.
5. Fu, Y., Li, H., and Yang, Z. (2002). The ROP2 GTPase controls the formation of cortical fine F-actin and the early phase of directional cell expansion during *Arabidopsis* organogenesis. Plant Cell *14*, 777–794.
6. Bloch, D., Lavy, M., Efrat, Y., Efroni, I., Bracha-Drori, K., Abu-Abied, M., Sadot, E., and Yalovsky, S. (2005). Ectopic expression of an activated RAC in *Arabidopsis* disrupts membrane cycling. Mol. Biol. Cell *16*, 1913–1927.
7. Fu, Y., Gu, Y., Zheng, Z., Wasteneys, G., and Yang, Z. (2005). *Arabidopsis* interdigitating cell growth requires two antagonistic pathways with opposing action on cell morphogenesis. Cell *120*, 687–700.
8. Gu, Y., Fu, Y., Dowd, P., Li, S., Vernoud, V., Gilroy, S., and Yang, Z. (2005). A Rho family GTPase controls actin dynamics and tip growth via two counteracting downstream pathways in pollen tubes. J. Cell Biol. *169*, 127–138.
9. Jones, M.A., Shen, J.-J., Fu, Y., Li, H., Yang, Z., and Grierson, C.S. (2002). The *Arabidopsis* Rop2 GTPase is a positive regulator of both root hair initiation and tip growth. Plant Cell *14*, 763–776.
10. TerBush, D.R., Maurice, T., Roth, D., and Novick, P. (1996). The Exocyst is a multiprotein complex required for exocytosis in *Saccharomyces cerevisiae*. EMBO J. *15*, 6483–6494.
11. Guo, W., Tamanoi, F., and Novick, P. (2001). Spatial regulation of the exocyst complex by Rho1 GTPase. Nat. Cell Biol. *3*, 353–360.
12. Wiederkehr, A., Du, Y., Pypaert, M., Ferro-Novick, S., and Novick, P. (2003). Sec3p is needed for the spatial regulation of secretion and for the inheritance of the cortical endoplasmic reticulum. Mol. Biol. Cell *14*, 4770–4782.
13. Novick, P., and Guo, W. (2002). Ras family therapy: Rab, Rho and Ral talk to the exocyst. Trends Cell Biol. *12*, 247–249.
14. Dvorsky, R., Blumenstein, L., Vetter, I.R., and Ahmadian, M.R. (2004). Structural insights into the interaction of ROCKI with the switch regions of RhoA. J. Biol. Chem. *279*, 7098–7104.
15. Alonso, J.M., Stepanova, A.N., Leisse, T.J., Kim, C.J., Chen, H., Shinn, P., Stevenson, D.K., Zimmerman, J., Barajas, P., Cheuk, R., et al. (2003). Genome-wide insertional mutagenesis of *Arabidopsis thaliana*. Science *301*, 653–657.
16. Benjamins, R., Quint, A., Weijers, D., Hooykaas, P., and Offringa, R. (2001). The PINOID protein kinase regulates organ development in *Arabidopsis* by enhancing polar auxin transport. Development *128*, 4057–4067.
17. Aida, M., Beis, D., Heidstra, R., Willemsen, V., Blilou, I., Galinha, C., Nussaume, L., Noh, Y.S., Amasino, R., and Scheres, B. (2004). The PLETHORA genes mediate patterning of the *Arabidopsis* root stem cell niche. Cell *119*, 109–120.
18. Bracha-Drori, K., Shichrur, K., Katz, A., Oliva, M., Angelovici, R., Yalovsky, S., and Ohad, N. (2004). Detection of protein-protein interactions in plants using bimolecular fluorescence complementation. Plant J. *40*, 419–427.
19. Lavy, M., Bracha-Drori, K., Sternberg, H., and Yalovsky, S. (2002). A cell-specific, prenylation-independent mechanism regulates targeting of type II RACs. Plant Cell *14*, 2431–2450.
20. Lavy, M., and Yalovsky, S. (2006). Association of *Arabidopsis* type-II ROPs with the plasma membrane requires a conserved C-terminal sequence motif and a proximal polybasic domain. Plant J. *46*, 934–947.
21. Sorek, N., Poraty, L., Sternberg, H., Bar, E., Lewinsohn, E., and Yalovsky, S. (2007). Activation status-coupled transient S acylation determines membrane partitioning of a plant Rho-related GTPase. Mol. Cell. Biol. *27*, 2144–2154.
22. Elias, M., Drdova, E., Ziak, D., Bavlnka, B., Hala, M., Cvrckova, F., Soukupova, H., and Zarsky, V. (2003). The exocyst complex in plants. Cell Biol. Int. *27*, 199–201.
23. Cole, R.A., Synek, L., Zarsky, V., and Fowler, J.E. (2005). SEC8, a subunit of the putative *Arabidopsis* exocyst complex, facilitates pollen germination and competitive pollen tube growth. Plant Physiol. *138*, 2005–2018.
24. Zhang, X., Bi, E., Novick, P., Du, L., Kozminski, K.G., Lipschutz, J.H., and Guo, W. (2001). Cdc42 interacts with the exocyst and regulates polarized secretion. J. Biol. Chem. *276*, 46745–46750.
25. Roumanie, O., Wu, H., Molk, J.N., Rossi, G., Bloom, K., and Brennwald, P. (2005). Rho GTPase regulation of exocytosis in yeast is independent of GTP hydrolysis and polarization of the exocyst complex. J. Cell Biol. *170*, 583–594.
26. Synek, L., Schlager, N., Elias, M., Quentin, M., Hauser, M.T., and Zarsky, V. (2006). AtEXO70A1, a member of a family of putative exocyst subunits specifically expanded in land plants, is important for polar growth and plant development. Plant J. *48*, 54–72.
27. Zuo, X., Zhang, J., Zhang, Y., Hsu, S.C., Zhou, D., and Guo, W. (2006). Exo70 interacts with the Arp2/3 complex and regulates cell migration. Nat. Cell Biol. *8*, 1383–1388.
28. Benkova, E., Michniewicz, M., Sauer, M., Teichmann, T., Seifertova, D., Jurgens, G., and Friml, J. (2003). Local, efflux-dependent auxin gradients as a common module for plant organ formation. Cell *115*, 591–602.
29. Geldner, N., Anders, N., Wolters, H., Keicher, J., Kornberger, W., Muller, P., Delbarre, A., Ueda, T., Nakano, A., and Jurgens, G. (2003). The *Arabidopsis* GNOM ARF-GEF mediates endosomal recycling, auxin transport, and auxin-dependent plant growth. Cell *112*, 219–230.
30. Xu, J., and Scheres, B. (2005). Dissection of *Arabidopsis* ADP-RIBOSYLATION FACTOR 1 function in epidermal cell polarity. Plant Cell *17*, 525–536.